ARMA 20–1411

Temperature and Pressure Profiles for Geothermal Battery Energy Storage in Sedimentary Basins

Palash Panja[1,2], John McLennan[1], Sidney Green[3,4]

[1]*Department of Chemical Engineering, University of Utah, Salt Lake City, Utah, United States*

[2]*Energy & Geoscience Institute, University of Utah, Salt Lake City, Utah, United States*

[3]*Enhanced Production, Inc., Salt Lake City, Utah, United States*

[4]*Research Professor, University of Utah, Salt Lake City, Utah, United States*

ABSTRACT:

Solar and wind power are being introduced into electric grids to supplement and replace conventional electricity. Unfortunately, the deployment of utility-scale storage has not kept pace with the variable nature of solar and wind. Cost effective large-scale energy storage is required for additional solar and wind renewable energies. The Geothermal Battery Energy Storage concept has the potential to provide this large-scale energy storage using a renewable energy source.

The concept uses solar radiance to heat water on the surface and then inject this heated water deep into the earth. This hot water would elevate the formation temperature creating a high temperature "geothermal reservoir" acceptable for conventional geothermal energy recovery. The unique feature is the use of sedimentary basins with high porosity and high permeability, at depths great enough to allow high temperature water injection and production. The process uses the produced formation water; and thus, neither fresh water nor surface storage or disposal of water is required. Furthermore, calculations show that nearly one hundred percent of the heat injected can be recovered for certain reservoirs.

Since there are many parameter variations possible for different reservoirs and injection-production cases, calculations are needed to consider the effects. This paper presents parametric calculations for permeability, porosity, reservoir thickness, injection rate, and other variables. Temperature and reservoir pressure profiles at distances away from the injection well and the production well are shown. For the calculations, the reservoir is considered to be homogeneous but with different horizontal to vertical permeabilities. Total heat recovered is shown for different parameter variations and different number of cycles of injection-production.

Key parameter effects on the produced water temperature and on the injection and production pressures are discussed. Being able to recover nearly one hundred percent of the heat injected dramatically increases the potential for large-scale thermal energy storage for daily, monthly, or even seasonal cyclic electric generation.

1. INTRODUCTION

Early concept evaluation has suggested that large-scale energy storage may be possible by storing solar thermal heat in the earth during periods of adequate solar radiance [1, 2]. This heat could then be extracted when energy is needed. Previous work [3-6] suggested that the efficiency of heat injected to heat extracted might be too low for practicality. However, the NSF funded SedHeat Geothermal Energy Project [7, 8] advocated to use solar thermal energy to heat water on the surface and inject the hot water into an appropriate sedimentary environment.

Recently, a team led by Idaho National Laboratory [2, 9] performed initial, high-level calculations to assess this concept. These ideal calculations showed that high permeability and porosity formations could provide storage media for injection of solar heated water, with subsequent production.

These calculations have been extended in the present work to focus on the quality of the reservoir that is required to enable feasibility. Some of the relevant parametric calculations done in the current work are presented to highlight the consequences of variations of basic reservoir parameters. Temperature and reservoir pressure profiles are shown along trajectories away from an injection/production well combination. These profiles represent different cyclic injection and production cases. The parameters varied include reservoir permeability and porosity for reservoirs of different thicknesses. Formation thermal conductivity and specific heat are also varied, as are injection and production rate. In all cases, the reservoir is considered to be homogeneous, except for horizontal to vertical permeability variation. Total heat recovered is also shown for selected reservoir scenarios and varying cycles of injection-production. Partial completion, while certainly significant, was not considered.

Concepts for exploiting thermal storage for a geothermal battery are summarized elsewhere [10]. A commercially viable operation would require a network of injectors and producers. To highlight the role of the reservoir itself in the simulations highlighted here, only one well is involved, conceptually serving as an injector-producer combination (in reality, two twinned wells might be required with different completions).

A commercial thermal simulator is used to study the effect of coupled thermal-fluid movement including convective heat transfer and heat conduction within the rock.

2. RESERVOIR MODEL AND SIMULATION

The coupled fluid flow and heat flow in the storage reservoir are numerically simulated using a thermal simulator from the Computer modeling group (CMG), Calgary, Canada. A 3D cylindrical (RZ) model of the reservoir is created as shown in Figure 1.

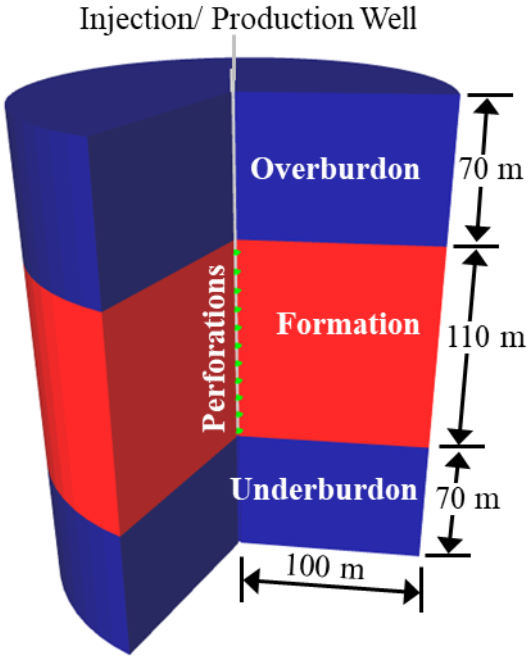

Fig. 1. Three-dimensional cylindrical (R-Z) model of the reservoir showing the three segments namely overburden, formation and underburden.

As can be seen in Figure 1, the thermal storage domain has three generic components: namely the insulating overburden at the top, the thermal "battery" in the middle (target formation) and the insulating underburden section at the bottom. There are 25 grids (layers) in the vertical direction. Each vertical layer is 10 meters thick. The overburden and underburden have 7 grids each which make each layer 70 meters thick. The formation has 11 layers making it 110 meters thick. Each layer has the same grid refinement in the radial and angular directions.

Results from constant pressure boundary conditions are considered here for a homogeneous reservoir, i.e., the parameters are spatially constant. The porosity and permeability of both the overburden and underburden sectors are kept very low; at 2.5% and 100 nD, respectively. The base case parameters are shown in Table 1.

Table 1: Base case parameters for the target formation, overburden and underburden

Parameters	Formation	Overburden/ Underburden
Specific heat of rock (J/(kg-K)	930	770
Thermal Conductivity (W/(m-K)	2.5	1.05
Density (kg/m^3)	2000	2500
Horizontal permeability, k_x, k_y (mD)	100	0.0001
Vertical permeability, k_z (mD)	10	0.0001
Porosity (%)	15	2.5
Initial Temperature (^{O}C)	120	120
Initial Pressure (MPa)	12	12
Thickness (m)	110	70

3. OPERATING SCHEDULE

In the simulated huff-and-puff scheme, hot water is injected for 8 hours at 250 ^{O}C. The water is then produced for 10 hours and finally, the well is shut-in for 6 hours before the next cycle starts. The entire schedule is based on a one-day (24 hr) cycle and in all cases, the volume of fluid injected equals the volume of fluid produced. The same schedule is repeated every day.

In most cases, the simulation considers 30 cycles; i.e., nominally one month. The base case has been run for 100 cycles to investigate the long-run impact on temperature, pressure and heat loss. The selected injection rate is 40 kg/second for an 8-hour injection. The production rate is 32 kg/second for a 10-hour cycle to keep the total produced water the same as the total injection water.

4. SENSITIVITY STUDY

The effects of different parameters are investigated in this single spot simulation suite ("huff and puff"). Single well injection and production is only the first step in considering site suitability. In reality, multiple injectors

and producers are required to commercially implement a geothermal battery concept. For example, as hot water is produced to generate power, water leaving the plant (binary or flash) will need to be reinjected. Over time, injector-producer configuration could vary. This is outside of the scope of this publication. Requirements for future study include partial penetration and partial completion and convective flow associated with these geometric configurations. Multiple layers and potential crossflow are also relevant for the design process.

Thermophysical parameters are considered; thermal conductivity and specific heat of the formation and intrinsic fluid. Formation transport and storage properties considered included permeability, porosity, and formation compressibility, as well as thickness. The fluid properties were based on a conventional equation of state for density (and hence compressibility) as well as accepted relationships for water viscosity. Operating conditions, (injection rates and times). Results from of a selection of these simulations are presented. The range of the selected parameters considered in the simulations is listed in Table 2. Simulation number 1 is considered as the base case. These values are chosen from the literature [9].

Table 2: List of simulations for sensitivity analysis of thermophysical and geologic properties of rock, fluid property, and operating parameter.

Scenario	Injection Rate (kg/s)	Permeability (mD)	Thickness (m)	Porosity (%)
1 (base case)	40	100	110	15
2	40	10	110	15
3	40	20	110	15
4	40	50	110	15
5	60	100	110	15
6	80	100	110	15
7	40	100	50	15
8	40	100	80	15
9	40	100	110	5
10	40	100	110	10
11	40	100	110	20

5. RESULTS

Spatio-temporal changes in temperature and pressure in the reservoir are analyzed to investigate the effects of different parameters. We have plotted the temperature and pressure changes with time (or cycle) at mid-height of the reservoir. In a second generic plot, temperature and pressure at the end of injection, the end of production and the end of shut-in are plotted along a radial path on a horizontal plane in the middle of the formation.

The results from the base case with 100 operating cycles (equivalent to 100 days of operation) are discussed first. The sensitivity studies, i.e., the effect of different parameters are discussed later for scenarios with 30 operating cycles.

5.1. Base Case

The parameters for the base case are listed in Table 1. The calculated temperature and profiles for 100 cycles are shown in Figure 2. The temperature is prescribed at 250^{O}C during injection and it drops to a lower temperature during production and stays there during shut-in. After each cycle, the temperature at the end of production and during shut-in increases. However, the produced water temperature reaches a rellatively constant value of 230 ^{O}C after about 70 cycles. Therefore, the production temperature at the midpoint of formation never reaches the injection temperature. Wellbore thermal effects are not considered and the pressure is maintained high enough for single-phase behavior. The difference between the injected water temperature and the produced water temperature is caused by the mixing of injection water at 250^{O}C with the initial reservoir water at 120^{O}C and exposure to a large, initially cooler reservoir. These effects cause the temperature near the mixing front to drop below 250^{O}C.

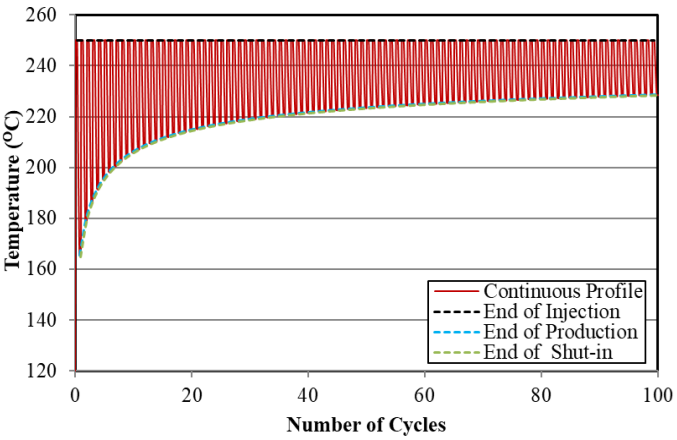

Fig. 2. Temperature at the middle of the formation for 100 cycles. Notice constant injection temperature of 250°C and a reduced but progressively increasing producing temperature

Since the same volume of water is produced as injected, hot water is initially produced from the near-wellbore zone; lower-temperature water - far from the wellbore - is produced later in the production stage. There is also heat conduction through the rock. Heat convection is limited or absent during shut-in and the only heat transfer occurs through the slow heat conduction. For this reason, the shut-in temperature in the middle of the formation stays constant for 6 hours.

The pressure profiles during injection, production, and shut-in are almost flat after around ten cycles as shown in Figure 3.

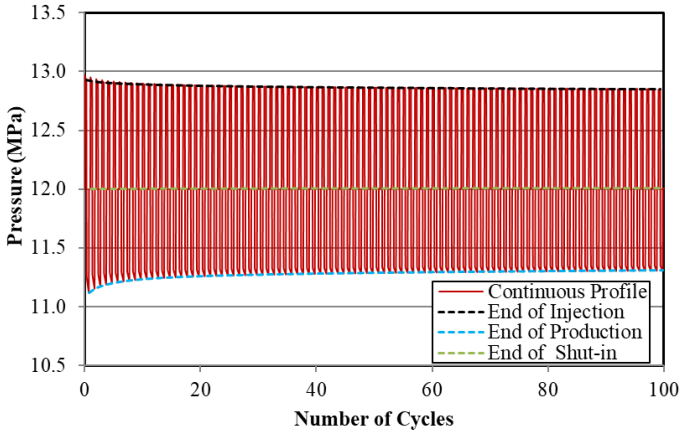

(a)

Fig. 3. Pressure at the middle of the formation for 100 cycles

Injection of 40 kg/s of water requires ~12.8 MPa of pressure; i.e., 0.8 MPa pressure above the initial reservoir pressure of 12 MPa. The production pressure drops to 11.3 MPa to produce the same rate of water because of the lower instantaneous volumetric flow rate. During shut-in, the pressure goes back to the initial reservoir pressure at 12 MPa because the constant pressure boundary condition "heals" the reservoir to reach pressure equilibrium faster than occurs for no-flow boundaries.

The temperature profiles along the radial path after the end of injection, end of production and end of a shut-in for different cycles (from cycle 1 to 100) are shown in Figure 4.

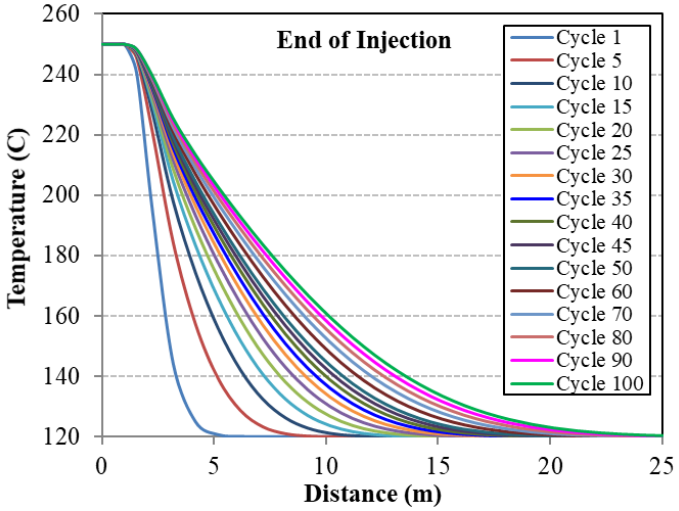

(a)

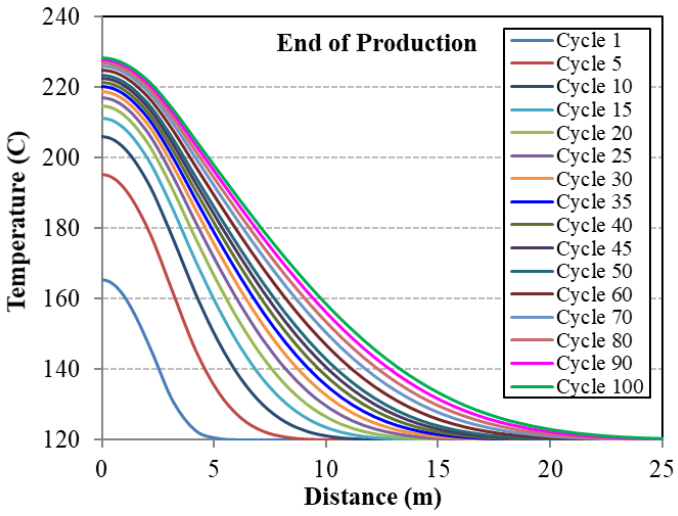

(b)

Fig. 4. Temperature along a radial path (this is axisymmetric) on a horizontal plane at the mi-height of the target formation at the (a) end of injection (b) end of production

The temperatures at the wellbore after the end of injection (in all cycles) are at 250 ^{O}C which is the temperature of the injected water (Figure 4a). However, as we move away from the wellbore, the temperature drops quickly to the initial reservoir temperature. In the first cycle, injected water "reaches" only 5 meters of cylindrical volume from the wellbore. Therefore, the bulk of the reservoir remains at initial temperature conditions beyond 5 meters at the end of the injection during the first cycle. This distance increases with each cycle and it is about 25 meters after 100 cycles of operation.

The affected reservoir volume at the end of production (Figure 4b) is similar to the injection volume, as discussed earlier. The temperature at the end of production increases with each cycle. In the first cycle, the temperature at the wellbore is about 165 ^{O}C whereas it is ~228 ^{O}C in the 100th production cycle. Similar behavior is observed in the case of a shut-in. This is because of the heating of the reservoir by the hot injected water at the starting of each cycle. The changes in temperature profile after each cycle are not linearly proportional to the cycle number. As would be expected, a greater difference is observed between cycle 1 and cycle 5 than between cycle 5 to cycle 10. The differences slowly diminish with the number of cycles. Very small differences are noticed after 70 cycles. Initially, the temperature difference between the injected water and the reservoir is higher. This driving force (temperature difference) becomes negligible as the cycles increase. The shut-in temperatures in each cycle are a little less than the production temperature. This is due to the slow heat conduction during shut-in.

The pressure profiles along a radial path at the end of injection and end of production are shown in Figure 5.

At the wellbore, the injection pressure is about 12.9 MPa and at the boundary, it is 12 MPa (virgin reservoir

pressure). In the case of production, wellbore pressure drops to 11 MPa because of the mass flow rate specified. During shut-in, the reservoir regains the initial pressure conditions at 12 MPa. No discernible differences among pressure profiles with different cycles are observed in all cases. Due to the constant pressure (12 MPa) boundary condition, the pressure remains at 12 MPa at the end of the radial path. After each cycle, the same volume of water is produced as was injected.

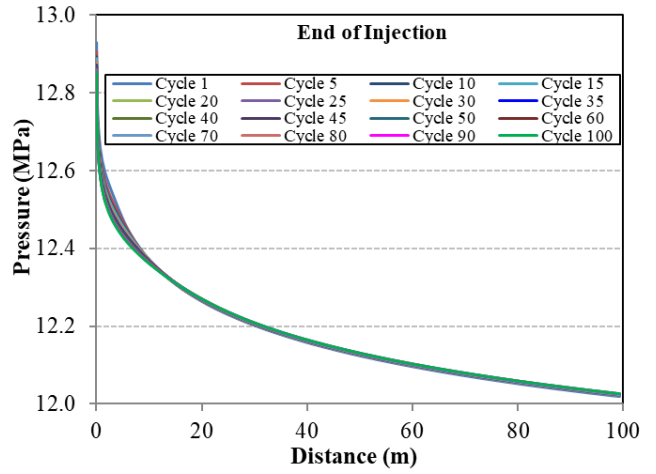

(a)

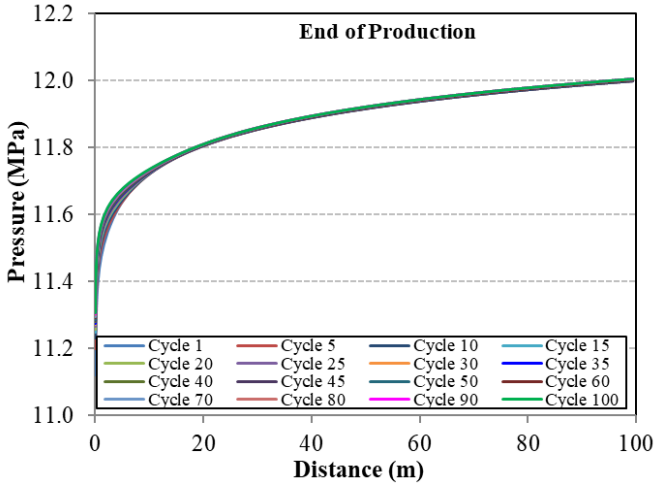

(b)

Fig. 5. Pressure along a radial path in the horizontal plane at the mid-height of the target formation after (a) end of injection (b) end of production

Beyond the temperature and pressure, heat recovery is the primary factor reflecting on the feasibility of the process of energy storage in a reservoir. Instead of heat recovery, heat loss in the reservoir is calculated in two ways; loss in an individual cycle and cumulative loss. The energy loss is calculated as follows.

$$Energy\ Loss\ (\%) = \frac{Energy\ In - Energy\ Out}{Energy\ In}\ X\ 100$$

The energy in the fluid (water) in the simulator is referred to as the enthalpy of the fluid using a reference temperature of 25^{O}C. The energy loss per cycle is shown in Figure 6.

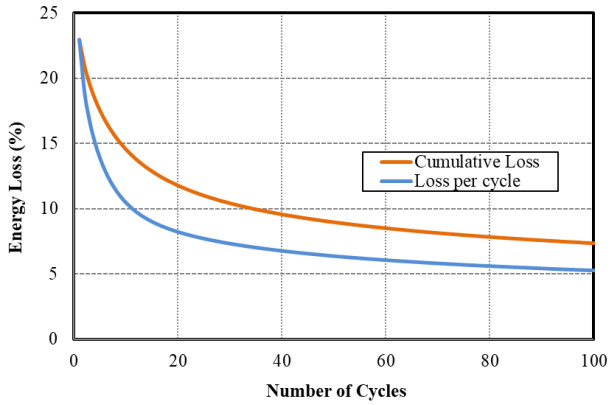

Fig. 6. Cumulative heat loss and loss per cycle

Initially, energy loss decreases drastically and then drops at a slow pace. For example, the cumulative loss drops from 23% in the first cycle to half to 11.8% in the 20th cycle. However, in the 40th cycle, the cumulative loss is about 10%. After 40 cycles, the overall energy loss decreases slowly as is evident from the asymptotic behavior in Figure 6. Energy loss in an individual cycle reaches about 5% after about 100 cycles or after more than 3 months of operation whereas cumulative energy loss is about 7% at the same time. In the base case, we have discussed the temperature and pressure profiles and the heat loss for different numbers of cycles. In the following sections, the effects of different parameters on these profiles are introduced.

5.2. Effect of Permeability

Absolute permeability is one of the relevant geologic parameters for fluid flow in porous media. The effects of permeability on temperature, and pressure are discussed here. Temperature profiles along a radial path at the mid-height of formation after the end of injection and end of production are shown in Figure 7 for a range of permeabilities.

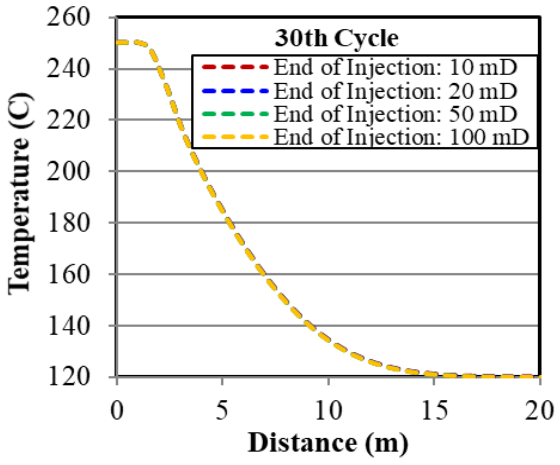

(a)

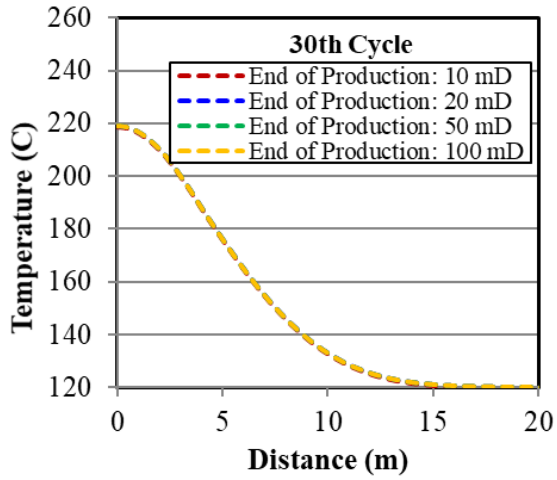

(b)

Fig. 7. Temperature profile along a radial path in the 30th cycle for permeabilities of 10, 20, 50 and 100 mD (a) end of injection (b) end of production

Despite simulating a 100-meter reservoir radius, temperature versus radial distance is plotted for 20 meters only, due to the limited propagation of the thermal front in the reservoir. This is due the poor conductive heat transfer between injected water and rock and in-situ water. The temperature front is dominated by the amount of hot water (250°C) injected and the mixing with the in-situ water at 120°C. While the thermal front is insesntive to pressure, the pressure profiles are naturally controlled by permeability. Pressure profiles after injection, production, and shut-in during the 30th cycle are shown in Figure 8.

The pressure fronts in all cases reach the boundaries which were maintained at constant pressure at 12 MPa. Higher pressure is required to inject same amount of water in lower permeability reservoir as expected due to higher resistance to flow in porous media. Similarly, lower bottom hole pressure is observed during production of the same amount of water to increase the drawdown.

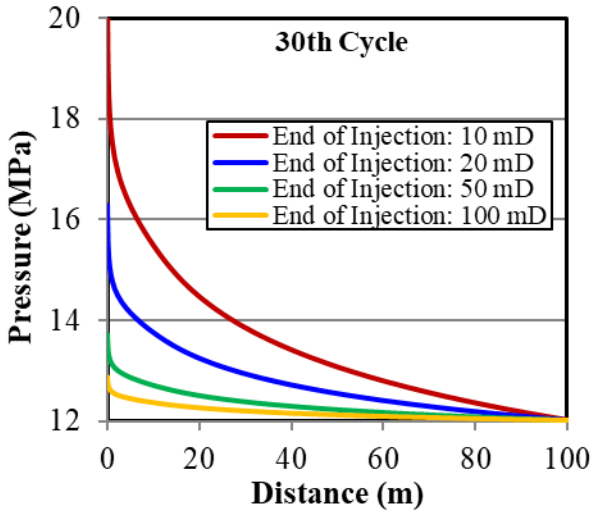

(a)

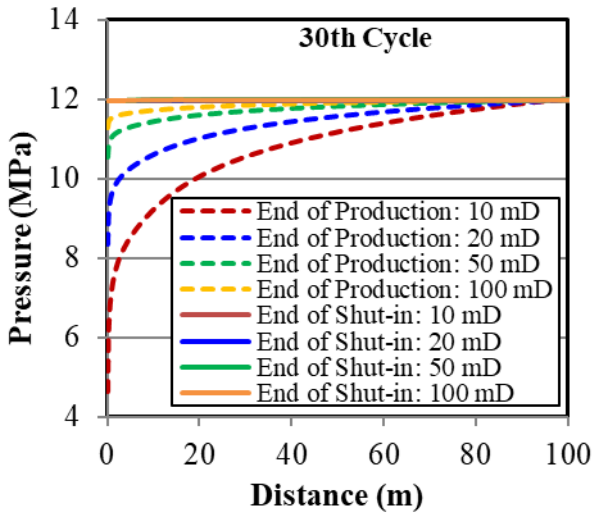

(b)

Fig. 8. Pressure profiles along a radial path in 30th cycle for permeabilities of 10, 20, 50 and 100 mD (a) end of injection (b) end of production and end of shut-in

5.3. *Effect of Injection Rate*

The injection rate is a vital operational parameter. The effects of the injection rate on temperature, and pressure are discussed here. Temperature profiles along a radial path at the mid-height of the target formation - after the end of injection and end of production - are shown for different injection rates in Figure 9. As no surprise, the injection rate has a prominent impact on the temperature inside the reservoir. A higher injection rate ensures that a greater volume of hot water is placed in the formation because the time of injection is always the same; i.e., 8 hours for all rates. Therefore, more heat is pumped into the formation with a higher injection rate. The mixing front also moves farther in this case, for the same reason. Consequently, a higher temperature is observed at the end of production for higher injection rates because the formation is heated to higher temperatures compared to lower injection rates. The heat content is greater in the influenced region of the reservoir.

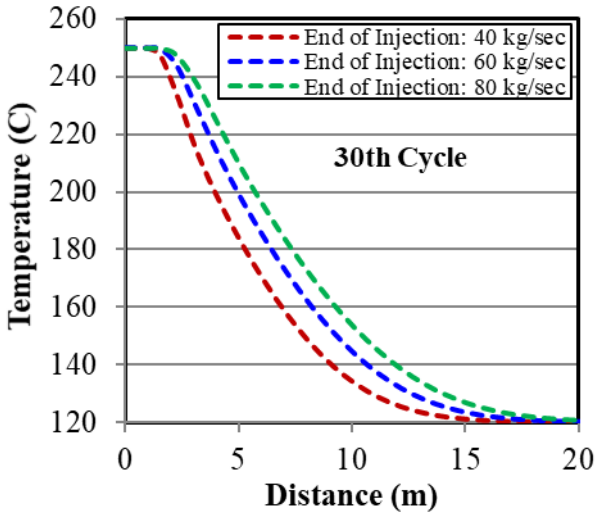

(a)

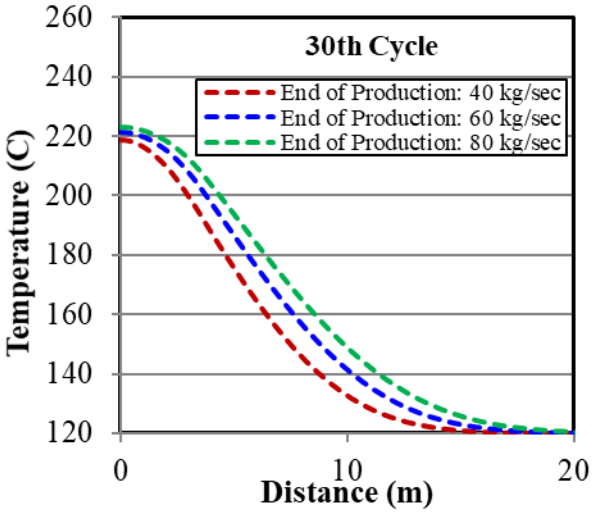

(b)

Fig. 9. Temperature profiles along a radial path in the thirtieth cycle for injection rates of 40, 60, and 80 kg/sec (a) end of injection (b) end of production.

The pressure profiles in the reservoir are greatly affected by the injection rate, as shown in Figure 10.

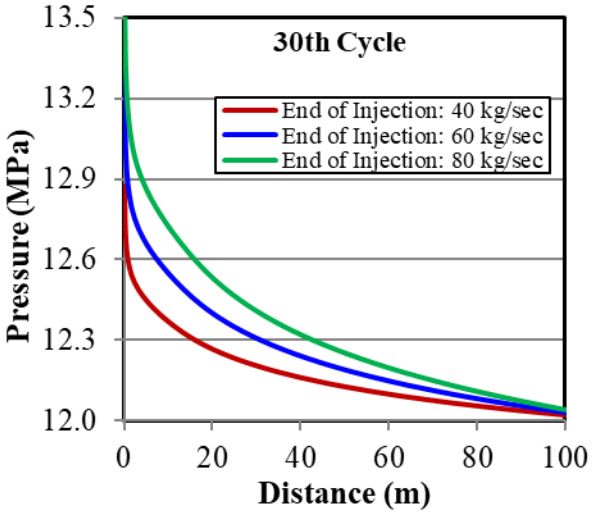

(a)

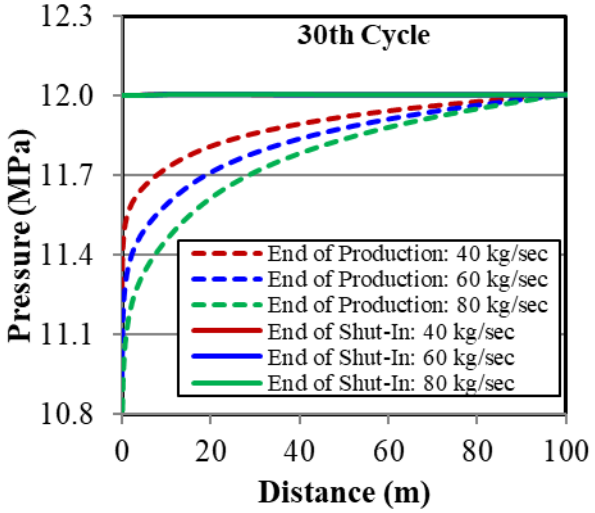

(b)

Fig. 10. Pressure profiles along a radial path in 30th cycle for the injection rates of 40, 60, and 80 kg/sec (a) end of injection (b) end of production and end of shut-in

Higher pressure is required to pump more water into the formation (simply Darcy's law). Hence, the pressure profile for the injection rate of 80 kg/sec lies above the other two profiles for injection rates of 60 and 40 kg/sec. On the other hand, greater drawdown is required to produce at a higher rate. Therefore, the pressure profile is lower for a higher rate during production. At shut-in, the pressure goes back to 12 MPa due to the support from constant pressure (12 MPa) boundary of the formation.

5.4. Effect of Formation Thickness

Formation thickness is considered to evaluate a reservoir's suitability as an energy storage system. A thin formation may not be a good candidate for various reasons such as heat loss from the top and bottom, higher injection pressure, less pore volume per meter from the wellbore, etc. The effects of three thicknesses, 50, 80 and 110 meters, are considered in terms of their effects on temperature, pressure and heat loss. The temperature and pressure profiles along a radial path at mid-height of the reservoir for the 30th cycle of operation for different thickness of the formation are shown in Figure 11 and Figure 12 respectively. The reader is referred to the solutions by Perkins and Gonzalez [11].

Simply following mass balance, a higher temperature is observed at the same radial location for a thin formation of 50 meters and vice versa if the formation is thicker. Recall that there is no partial completion skin (injection is over the full reservoir height).

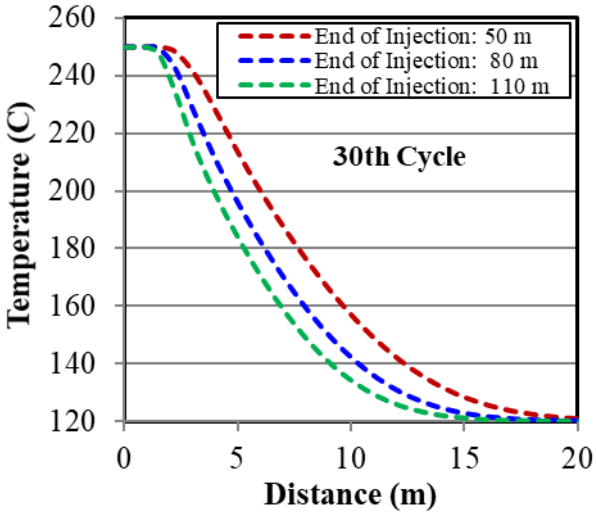

(a)

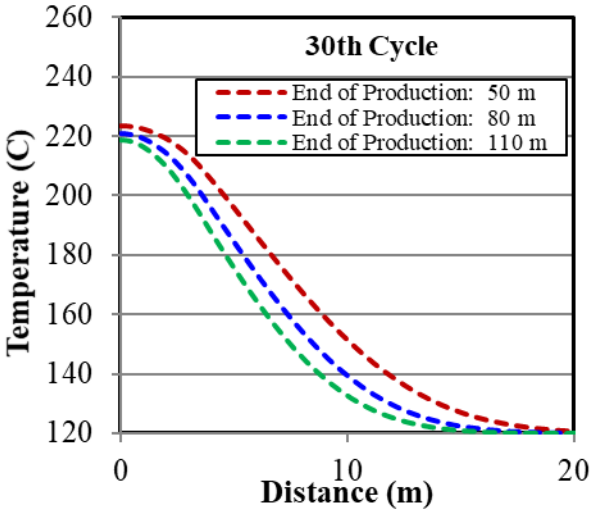

(b)

Fig. 11. Temperature profiles along a radial path in the 30th cycle for the formation thicknesses of 50, 80, and 110 meters (a) end of injection (b) end of production

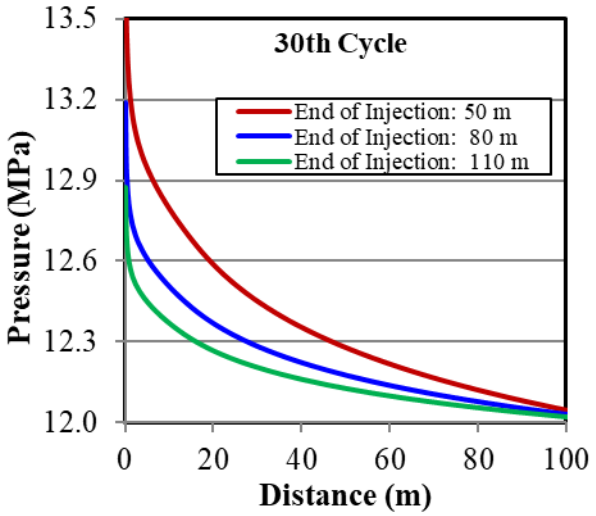

(a)

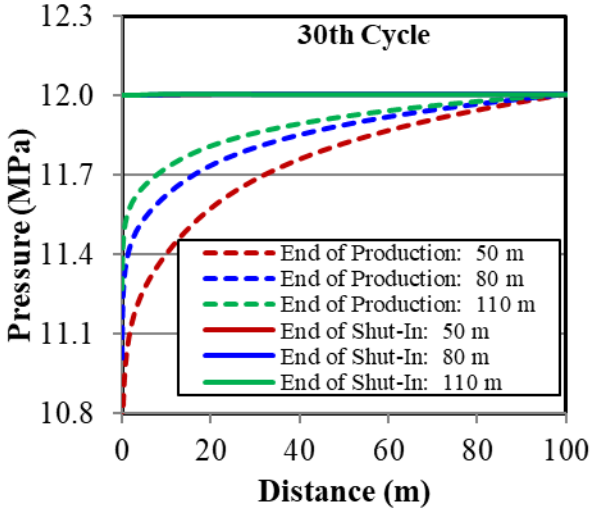

(b)

Fig. 12. Pressure profiles along a radial path in 30th cycle for the formation thicknesses of 50, 80, and 110 meters (a) end of injection (b) end of production and end of shut-in

A thicker formation has a greater pore volume for the same radius; i.e., more injected water can be accommodated for the same distance from the wellbore. On the other hand, for the injection of the same amount of water, the mixing front will move farther away from wellbore in the case of a thin formation. This will spread the hot water deeper into the reservoir. Therefore, the mixing front travels farther in a thin formation and the temperature is higher at the same radial location than in a thicker formation.

5.5. Effect of Formation Porosity

For porosity sensitivity studies, a lower value (5%) and a higher value (20%) were selected to bracket the base case (15%). With all other properties of rock and fluid the same, porosity has insignificant impact on the temperature and pressure profiles.In Figure 13, temperatures versus radial distance are shown for the 30th cycle with three different porosities.

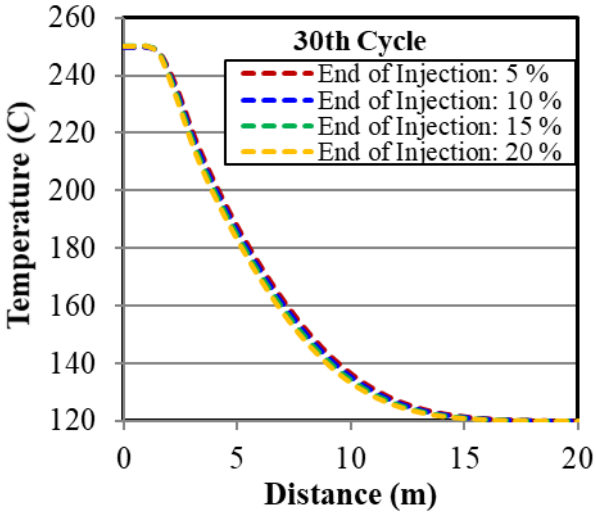

(a)

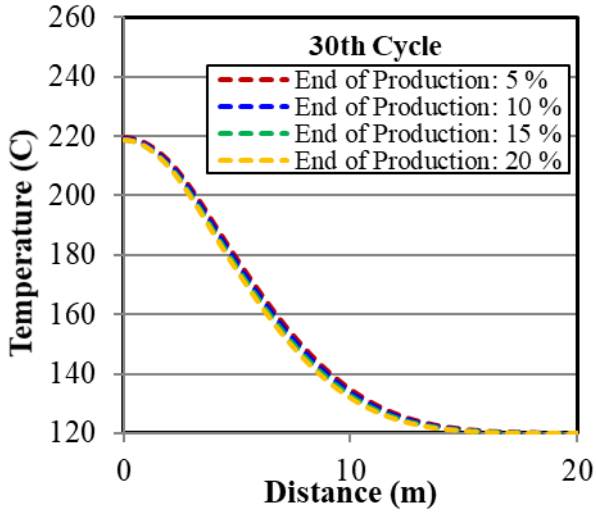

(b)

Fig. 13. Temperature profiles along a radial path for the 30th cycle for formation porosity of 5, 10, 15 and 20% (a) end of injection (b) end of production.

The impacts of porosity on pressure profiles are shown in Figure 14.

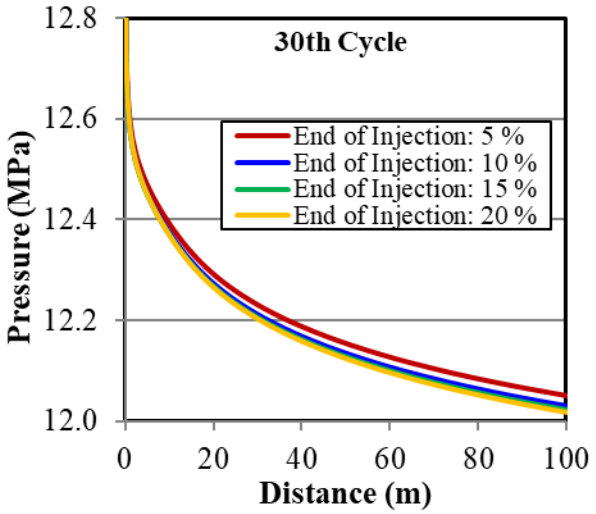

(a)

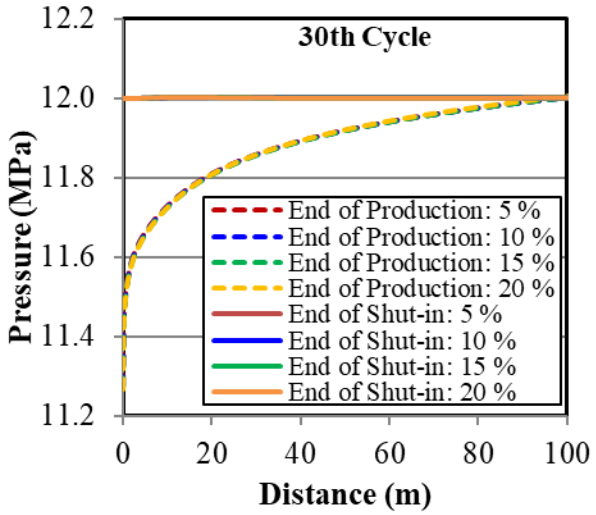

(b)

Fig. 14. Pressure profiles along a radial path in the 30th cycle for formation porosity of 5, 10, 15 and 20% (a) end of injection (b) end of production and end of shut-in.

The insignificant impact of porosity on pressure is anticipated. The permeability is high enough that the greater penetration of the fluid front does not significantly change the injection and production pressures (there is a radial logarithmic dependency). More intuitively surprising is the minor role that the porosity exerts on the temperature. The rationale is that mixing plays a dominant role; see for example, [11, 12, 13]. The analytical developments of Marx and Langenheim, 1959, [11] are particularly useful for demonstrating the muted influence of the porosity as a result of the heat transfer mechanisms. The formation rock also absorbs some heat from the hot injected water. Rock volume varies from 80% (for 20 % porosity) to 95% (5 % porosity) of the formation volume. Therefore, the hot water front only travels around 20 meters despite the pressure front reaches far deeper in the formation. Thus, the thermal profiles is also governed by the ratio of the specific heats of rock and water. The compressibility of water to accommodate the injected water is another factor in the movement of temperature front.

6. CONCLUSIONS

Thermal effects for injection and production of hot water into the earth are complicated and not always intuitive. Computer calculations show the complexity resulting from temperature variations that occur in the rock and the pore fluid within the rock.

From the calculations here, significant temperature variations progress only about twenty-five meters from the injection or production wellbore, even after many cycles of injection/production. Both temperatures and reservoir pressures tend to reach stable radial profiles after ten to twenty injection/production cycles. Permeability, porosity, injection/production rates, and cycles, and formation thickness (and to a lesser extent the specific heat of the rock) all affect the temperature and pressure profiles, and heat recovery efficiency.

For the calculations here, lower permeabilities lead to greater pressure during injection and a greater required drawdown for production, with a large effect occurring for permeabilities below about 50 millidarcies. As is well known, even from analytical solutions, lower reservoir thicknesses extend temperatures further from the wellbore and leads to higher bottom hole pressure cycles. Higher injection rates also tend to have about the same effect on temperature and pressure profiles as lower thickness reservoirs.

As is evident, and can be confirmed analytically, the thermal front does not advance a great distance into the reservoir. This is an operationally important consideration for well siting, to avoid injectate being captured by natural fractures and to find an adequately extensive, high permeability with significant net height.

In all cases, the heat recovery after a number of cycles tended to be high, over ninety percent per each cycle and, long-scale energy storage of daily to weekly or even seasonal cycles seems possible.

REFERENCES

1. McTigue, J., J. Castro, G. Mungas, N. Kramer, J. King, C. Turchi, and G. Zhu, Hybridizing a geothermal power plant with concentrating solar power and thermal storage to increase power generation and dispatchability. *Applied Energy*, 2018. 228.

2. Wendt, D., H. Huang, G. Zhu, P. Sharan, J. McTigue, K. Kitz, S. Green, and J. McLennan, Geologic Thermal Energy Storage of Solar Heat to Provide a Source of Dispatchable Renewable Power and Seasonal Energy Storage Capacity. *GRC Transactions*, 2019. 43.

3. US-DOE, Geo Vision—Harnessing the Heat Beneath our Feet. 2019.

4. Augustine, C. Design Requirements for Commercial Sedimentary Geothermal Projects. 2016. United States.

5. Burns, E., T.T. Cladouhos, C.F. Williams, and J. Bershaw, Controls on deep direct-use thermal energy storage (DDU-TES) in the Portland Basin, Oregon, USA. 2018.

6. Ueckert, M., R.L. Niessner, and T. Baumann. High Temperature Aquifer Storage, SGP-TR-209. in *Proceedings 41st Workshop on Geothermal Reservoir Engineering*, February 22-24. 2016. Stanford University.

7. Green, S. Unlocking the Energy Elephant—a SedHeat Workshop-Closing Comments. NSF Sponsored Workshop. University of Utah, Salt Lake City, 2017. March 1-4.

8. Green, S. Geothermal Battery Energy Storage. in SedHeat-ARMA Foundation *Pre-Concept Meeting*. 2017. San Francisco, June 24.

9. Wendt, D.S., H. Huang, G. Zhu, P. Sharan, J. McTigue, K. Kitz, S. Green, J. McLennan, and G.H. Neupane, Flexible Geothermal Power Generation utilizing Geologic Thermal Energy Storage: *Final Seedling Project Report*. 2019: United States.

10. Green, S., McLennan, J., Panja, P., Kitz, K., Allis, R., and J. Moore, Geothermal Battery Energy Storage, April 2020 (in preparation).

11. Marx, J.W., and R.H. Langenheim, Reservoir Heating by Hot Fluid Injection, SPE 1266-G, October 1959.

12. Perkins, T.K., and J.A. Gonzalez, Changes in Earth Stresses Around a Wellbore Caused by Radially Symmetrical Pressure and Temperature Gradients, SPE 10080, *SPEJ*, Vol. 24, Issue 02, April 1984.

13. Pratt, M., Thermal Recovery, SPE Monograph Series volume 7, 1982.